# Infrared and Raman spectra, conformational stability, ab initio calculations of structure and vibrational assignment of 4-fluoro-1-pentyne

**ARTICLE** *in* JOURNAL OF MOLECULAR STRUCTURE · SEPTEMBER 2003

Impact Factor: 1.6 · DOI: 10.1016/S0022-2860(03)00426-5



**4 AUTHORS**, INCLUDING:

Gamil A. Guirgis
College of Charleston
**341** PUBLICATIONS **2,688** CITATIONS

Available online at www.sciencedirect.com
SCIENCE DIRECT®
Journal of Molecular Structure 657 (2003) 271–289
Journal of MOLECULAR STRUCTURE
www.elsevier.com/locate/molstruc

# Infrared and Raman spectra, conformational stability, ab initio calculations of structure and vibrational assignment of 4-fluoro-1-pentyne

James R. Durig[a,*], Xiaodong Zhu[a,1], Gamil A. Guirgis[a], Stephen Bell[b]

[a]*Department of Chemistry, University of Missouri-Kansas City, Kansas City, MO 64110-2499, USA*
[b]*Department of Chemistry, University of Dundee, Dundee, Scotland DD1 4HN, UK*

Received 16 May 2003; accepted 17 June 2003

**Abstract**

The infrared spectra (3500–50 $cm^{-1}$) of the gas and solid and the Raman spectra (3500–50 $cm^{-1}$) of the liquid and solid have been recorded for 4-fluoro-1-pentyne, $HC \equiv CCH_2C(H)FCH_3$. All three expected conformers (*F-trans*, *H-trans* and *Me-trans* corresponding to the fluorine atom, hydrogen atom, and methyl group, *trans* to triple bond) have been identified in the fluid phases. Variable temperature studies of the infrared spectra (3500–400 $cm^{-1}$) of the sample dissolved in liquid krypton (−105 to −135 °C) have been recorded. Utilizing six sets of conformer pairs, the enthalpy differences have been determined to be 129 ± 13 $cm^{-1}$ (1.54 ± 0.16 kJ/mol) between the most stable conformer, the *F-trans* form, and the one of intermediate stability, the *H-trans* form and 178 ± 18 $cm^{-1}$ (2.13 ± 0.21 kJ/mol) between the *F-trans* form and the *Me-trans* conformer, the least stable form. At ambient temperature there is approximately 51% of the *F-trans* conformer, 27% of the *H-trans* conformer, and 22% of the *Me-trans* form present in the vapor state. In the polycrystalline state, the most stable conformer is the one with the hydrogen atom *trans* to the triple bond which is believed to result from crystal packing factors. Complete vibrational assignments are proposed for all three conformers based on infrared contours, relative intensities, depolarization values and group frequencies which are supported by the normal coordinate calculations utilizing the force constants from the ab initio MP2/6-31G(d) calculations. Complete equilibrium geometries have been determined for both rotamers by ab initio calculations employing a variety of basis sets at the level of Moller–Plesset with full electron correlation by the perturbation method to the second order (MP2) and by density functional theory utilizing the B3LYP method. From all of these calculations the *F-trans* conformer is predicted to be the most stable form, but the energy difference is significantly higher than the experimentally determined enthalpy difference. The results are discussed and compared to the corresponding quantities to those obtained for some similar molecules.


*Keywords:* Conformational stability; Krypton solution; Infrared and Raman spectra; Ab initio calculations; 4-Fluoro-1-pentyne

## 1. Introduction

We recently reported a conformational stability study of 1-pentyne, $CH_3CH_2CH_2C \equiv CH$, and

* Corresponding author. Tel.: +1-816-235-6038; fax: +1-816-235-2290.
*E-mail address:* durigj@umkc.edu (J.R. Durig).
[1] Taken in part from the dissertation of X. Zhu which will be submitted to the Department of Chemistry in partial fulfillment of the PhD degree.

0022-2860/03/$ - see front matter © 2003 Elsevier B.V. All rights reserved.
doi:10.1016/S0022-2860(03)00426-5

concluded that the *trans* conformer (methyl group *trans* to the triple bond) was the more stable form by $113 \pm 26\ cm^{-1}$ ($1.35 \pm 0.31$ kJ/mol) from a variable temperature infrared spectral study of a xenon solution [1]. The result was compared to the conformational stability of *n*-butane, $CH_3CH_2CH_2$-$CH_3$, where the *trans* form is more stable than the *gauche* conformer [2] by $234 \pm 33\ cm^{-1}$ ($2.80 \pm 0.39$ kJ/mol) since the 1-pentyne molecule simply results from the replacement of a methyl group in *n*-butane by the ethynyl group. In a recently reported electron diffraction study [3], it was concluded that the *gauche* conformer of 1-pentyne is the more stable rotamer by $18 \pm 44\ cm^{-1}$ with a composition of $68.6 \pm 4.5\%$ of the *gauche* conformer where the conclusion was supported by ab initio MP2/6-31G(d) calculations with the *gauche* form predicted to be more stable by $122\ cm^{-1}$. However this result has been challenged [4] based on the enthalpy determination from seven sets of conformer pairs from a xenon solution and ten sets of conformer pairs from a krypton solution with values of $50 \pm 6\ cm^{-1}$ ($0.60 \pm 0.07$ kJ/mol) and $45 \pm 4\ cm^{-1}$ ($0.54 \pm 0.05$ kJ/mol), respectively, with the *trans* conformer the more stable rotamer. This latter result for the xenon solution gives a smaller enthalpy value but is consistent with the earlier determinations where only three or four different temperatures were used which resulted in values of $101 \pm 52$, $111 \pm 55$, and $127 \pm 47\ cm^{-1}$ for the enthalpy difference [1]. These values except the last one, which was obtained from only three temperatures, are within the more recently reported value. Therefore, it is clear that 1-pentyne has the *trans* conformer as the more stable rotamer in the rare gas solutions and it is expected that the enthalpy value in the gas phase will be similar to the values in the rare gas solutions since they behave as pseudogases for conformers when they have similar volumes and dipole moments [5–8]. However, the ab initio calculations [4] with the relatively large basis set of 6-311 + G(2df,2pd) at the MP2 level gives incorrectly the *gauche* form the more stable confomer by $108\ cm^{-1}$.

We also investigated the enthalpy difference for the conformers of 4-fluoro-1-butyne, $HC \equiv CCH_2$-$CH_2F$, and determined that the *trans* conformer was more stable than the *gauche* form with $\Delta H$ values of $215 \pm 22$ ($2.57 \pm 0.26$ kJ/mol) and $170 \pm 17\ cm^{-1}$ ($2.04 \pm 0.2$ kJ/mol) from xenon and krypton solutions, respectively [9]. These results are in agreement with the ab initio predicted stability where three different basis sets at the MP2 level gave values ranging from a low value of 245 to a high value of $290\ cm^{-1}$, with the *trans* form the more stable conformer. The predicted stability from B3LYP/6-31G(d) calculations was slightly higher, with a value of $362\ cm^{-1}$. Thus, the average experimental enthalpy value is about $100\ cm^{-1}$ lower than the average predicted value for the energy difference for the conformers.

As a continuation of these conformational stability studies, we have investigated the 4-fluoro-1-pentyne, $HC \equiv CCH_2C(H)FCH_3$, molecule where there are three expected stable conformers, i.e. fluorine atom (*F-trans*), hydrogen atom (*H-trans*) and methyl group (*Me-trans*), *trans* to the triple bond. Based on the earlier studies cited above, one expects the *F-trans* conformer to be the most stable form, but it is not clear which of the other two conformers will be the next stable form. Therefore, we have obtained variable temperature FT-IR spectra of krypton solutions. Additionally, the infrared spectra of the gas and solid and the Raman spectra of the liquid and solid have been recorded. To support the spectroscopic studies, ab initio calculations have been carried out with a variety of basis sets at the level of the restricted Hartree–Fock (RHF) and with full electron correlation by the perturbation method [10] to the second order (MP2) to obtain the geometric parameters, harmonic force constants, infrared intensities, Raman activities, depolarization values and vibrational frequencies. Hybrid density function theory (DFT) calculations have also been carried out by the B3LYP method to obtain conformational energy differences and vibrational frequencies. The results of these spectroscopic and theoretical studies are reported herein.

## 2. Experimental

The 4-fluoro-1-pentyne sample was prepared from the corresponding alcohol, $HC \equiv CCH_2CH(OH)CH_3$, (Aldrich Chemical Co. Inc., Milwaukee, WI) utilizing (diethylamino) sulfur trifluoride (DAST), Aldrich

Chemical Co. at −60 °C. Purification was carried out by means of a low-temperature, low-pressure fractionation column and the purity was checked by infrared spectroscopy and stored under vacuum at low temperature until its use for the spectroscopic investigations.

The mid-infrared spectra of gaseous (Fig. 1A) and solid (Fig. 1B) 4-fluoro-1-pentyne were obtained with a Perkin–Elmer model 2000 Fourier transform spectrometer equipped with a Nichrome wire source, a Ge/CsI beamsplitter, and a DTGS detector. The spectrum of the gas (Fig. 1A) was obtained with the sample contained in a 10 cm cell fitted with CsI windows. The spectrum of the solid (Fig. 1B) was obtained by condensing the sample on a CsI substrate, held at ~77 K by boiling liquid nitrogen, housed in a vacuum cell fitted with CsI windows. The sample was condensed as an amorphous solid and repeatedly annealed until no further changes were observed in the spectrum. The theoretical resolution used to obtain the spectra of both the gas and the solid was 1.0 $cm^{-1}$.

The mid-infrared spectra of the sample, dissolved in liquified krypton (Fig. 2A) as a function of temperature, were recorded on a Bruker model IFS-66 Fourier transform spectrometer equipped with a Globar source, Ge/KBr beamsplitter, and a DTGS detector. The temperatures utilized ranged from −105 to −135 °C for the krypton solution. These studies were performed in a specially designed cryostat cell which consists of a 4 cm path-length copper cell with wedged silicon windows sealed to the cell with indium gaskets. The cell is cooled by boiling liquid nitrogen and the temperature is monitored with two Pt thermoresistors. The complete cell is attached to a pressure manifold to allow for the filling and evacuation of the cell. Once the cell is cooled to the desired temperature, a small amount of the sample is condensed into the cell. The cell is then pressurized with the noble gas, which immediately starts condensing in the cell, allowing the compound to dissolve. For each temperature investigated, 100 interferograms were recorded with a nominal resolution of 1.0 $cm^{-1}$, averaged, and transformed with a boxcar truncation function.

The Raman spectra of the liquid (Fig. 3A) and solid 4-fluoro-1-pentyne (Fig. 3B) were recorded on a SPEX model 1403 spectrophotometer equipped with a Spectra-Physics model 164 argon ion laser operating

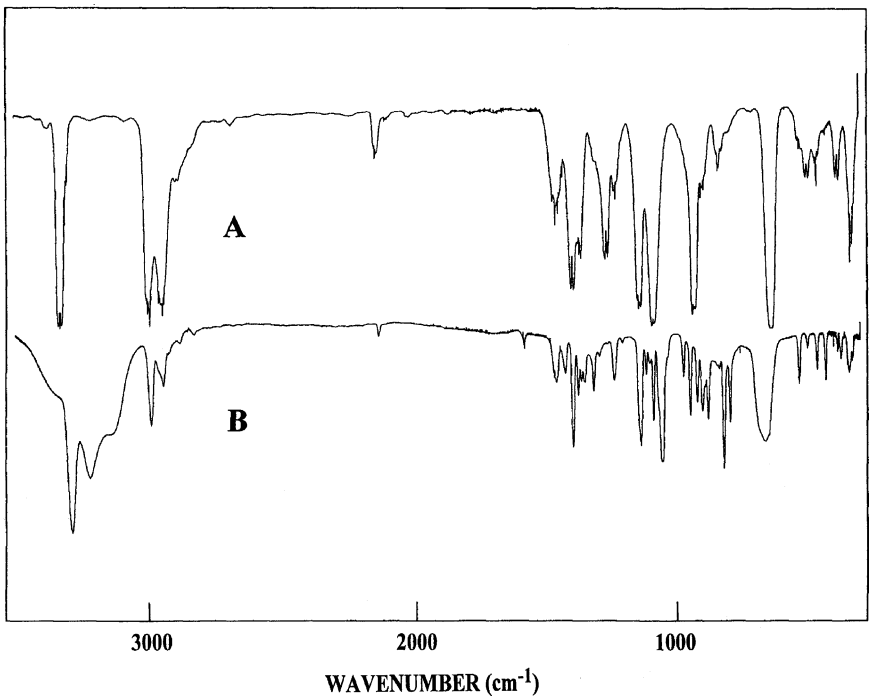


Fig. 1. Mid-infrared spectra of 4-fluoro-1-pentyne: (A) gas; and (B) annealed solid.

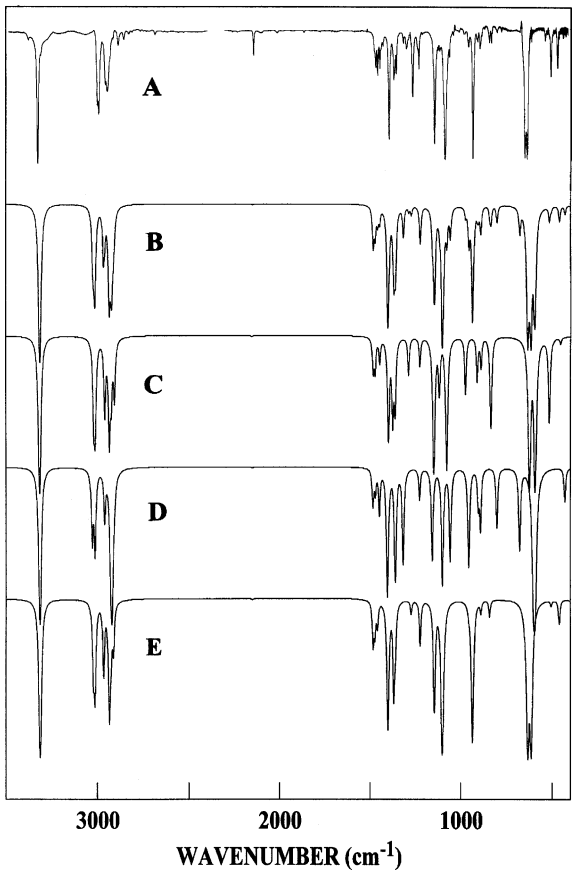


Fig. 2. Mid-infrared spectra of 4-fluoro-1-pentyne: (A) krypton solution at −125 °C; (B) simulated infrared spectrum of the *F-trans, H-trans* and *Me-trans* conformers mixture with a $\Delta H$ 129 and 178 $cm^{-1}$; (C) calculated for the pure *Me-trans* conformer; (D) calculated for the pure *H-trans* conformer; and (E) calculated for the pure *F-trans* conformer.

on the 5145 Å line. Laser power at the sample ranged from 0.4 to 1.0 W depending on the physical state of the sample. The spectrum of the liquid was recorded with the sample contained in a sealed capillary with a spherical bulb [11], while the spectrum of the liquid as a function of temperature and the spectrum of the solid were obtained using a Miller–Harney cell [12]. Multiple annealings were carried out in order to obtain the spectra of the polycrystalline solid.

The far infrared spectrum of the gas (Fig. 4A) was recorded on a Bomem model DA3.002 Fourier transform spectrometer equipped with a vacuum bench, 6.25 and 25 μm Mylar beamsplitters, and a liquid helium-cooled Si bolometer. The spectrum was obtained from the sample contained in a 1 m folded path cell equipped with mirrors coated with gold, and fitted with polyethylene windows with an effective resolution of 0.1 $cm^{-1}$. The far infrared spectra of the amorphous and annealed solids (Fig. 4B and C) were recorded on the previously described Perkin–Elmer model 2000 spectrometer. A grid beamsplitter and a cryostat cell with polyethylene windows were used and the sample was deposited on a silicon substrate at ~77 K. All of the pronounced infrared and Raman bands observed for 4-fluoro-1-pentyne are available from the authors and the observed fundamentals with their assignments for each of the conformers are listed in Tables 1–3.

## 3. Ab initio calculation

The LCAO-MO-SCF ab initio calculations were performed with the GAUSSIAN-98 program [13] using Gaussian type basis functions. The energy minima with respect to the nuclear coordinates were obtained by the simultaneous relaxation of all of the geometric parameters using the gradient method of Pulay [14]. Calculated energies were determined from MP2/6-31G(d), MP2/6-311 + G(2d,2p) and MP2/DZ(d) calculations, as well as six B3LYP calculations, and they are listed in Table 4. The geometrical parameters for the three stable conformers of 4-fluoro-1-pentyne from RHF, MP2, and B3LYP calculations are listed in Table 5.

In order to determine the degree of mixing and to obtain a more complete description of the molecular motions involved in the fundamentals of 4-fluoro-1-pentyne, a normal coordinate analysis has been carried out. The force field in Cartesian coordinates was calculated by the GAUSSIAN-98 program [13] at the MP2/6-31G(d) level. The following procedure was used to transform the ab initio results in Cartesian coordinates into symmetry coordinates. The Cartesian coordinates obtained for the optimized structure were input to a G-matrix program with a complete set of 33 internal coordinates (Fig. 5), which was used to form the symmetry coordinates (Table 6). The output of this G-matrix program consists of the B-matrix and the unsymmetrized G-matrix. The B-matrix was used to convert the ab initio force field in Cartesian coordinates to

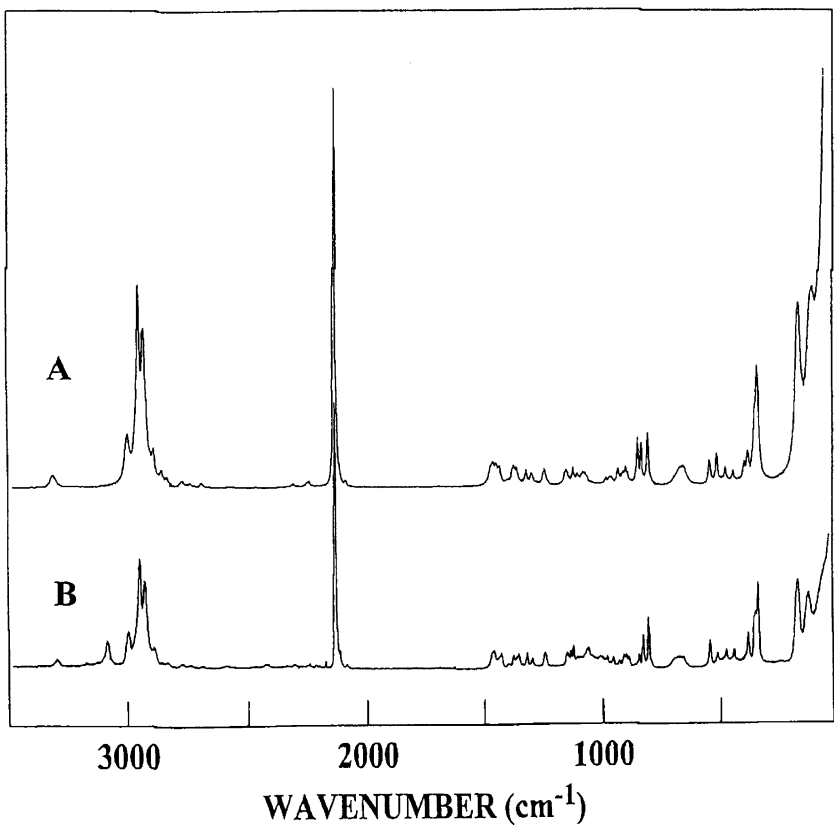


Fig. 3. Raman spectra of 4-fluoro-1-pentyne: (A) liquid; and (B) annealed solid.

a force field in internal coordinates [15]. The force fields for all three conformers can be obtained from the authors.

All the diagonal elements of the force fields in internal coordinates were assigned scaling factors. These force fields were then input, with the unsymmetrized G-matrix and scaling factors, to the perturbation. Initially, all the scaling factors were kept fixed at a value of 1.0 to produce pure ab initio calculated vibrational frequencies. For the force field obtained with the MP2/6-31G(d) basis set, scaling factors of 0.88 for the C–H stretches, 0.90 for the heavy atom stretches and C–H bends, except 1.3 for the C ≡ C–H bend, 1.5 for the C ≡ C–C bend, and 1.0 for all other coordinates, were utilized to obtain the 'fixed scaled' force field and resultant frequencies which are provided in Tables 1 (*F-trans*), 2 (*H-trans*) and 3 (*Me-trans*).

The Raman (Fig. 6) and infrared (Fig. 2) spectra for 4-fluoro-1-pentyne were predicted using 'fixed scaled' frequencies, scattering activities and infrared intensities determined from the GAUSSIAN-98 program [13] from the MP2/6-31G(d) calculations. The Raman scattering cross-sections, $\partial\sigma_j/\partial\Omega$, which are proportional to the Raman intensities, can be calculated from the scattering activities and the predicted frequencies for each normal mode [16,17]. To obtain the polarized Raman cross sections, the polarizabilities are incorporated into $S_j$ by $S_j[1-\rho_j/1+\rho_j]$, where $\rho_j$ is the depolarization ratio of the $j$th normal mode [18,19]. The Raman scattering cross-sections and the predicted scaled frequencies were used together with a Lorentzian function to obtain the calculated spectra.

Infrared intensities were calculated based on the dipole moment derivatives with respect to Cartesian

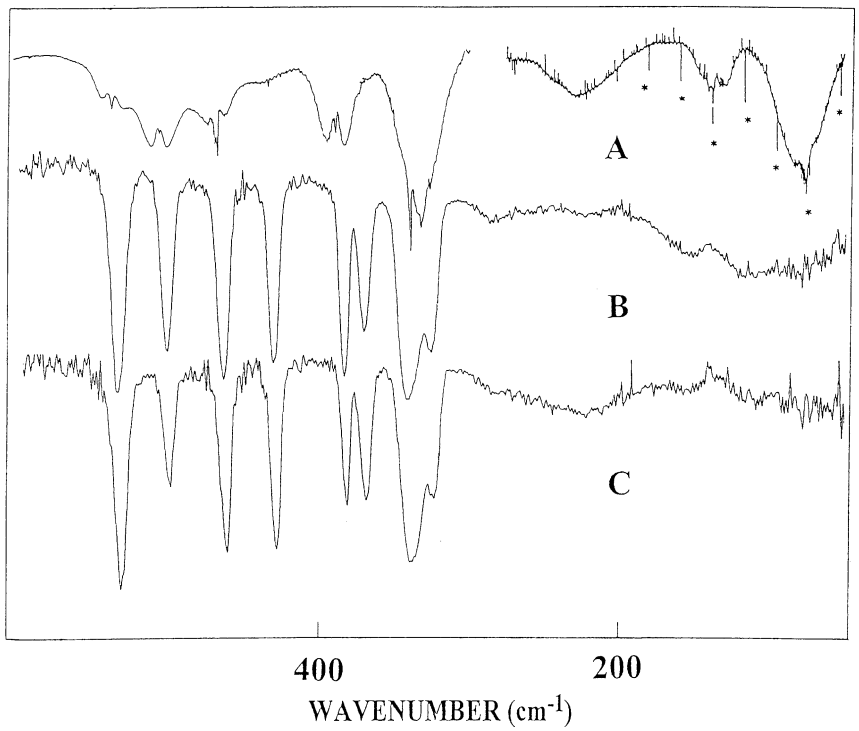


Fig. 4. Far-infrared spectra of 1-penten-4-yne: (A) gas; (B) amorphous solid; and (C) annealed solid.

coordinates. The derivatives were taken from the ab initio calculations and transformed to normal coordinates by

$$\left(\frac{\partial \mu_u}{\partial Q_i}\right) = \sum_j \left(\frac{\partial \mu_u}{\partial X_j}\right) L_{ij}$$

where the $Q_i$ is the $i$th normal coordinate, $X_j$ is the $j$th Cartesian displacement coordinate, and $L_{ji}$ is the transformation matrix between the Cartesian displacement coordinates and normal coordinates. The experimental Raman spectrum of the liquid and mid-infrared spectrum of the krypton solution for 4-fluoro-1-pentyne are included with the calculated spectra in Figs. 6A and 2A, respectively, for comparative purposes. The calculated spectra of the mixture of the three conformers were obtained using the enthalpy differences obtained from the temperature study of the liquid krypton solution (Table 7). The agreement between the calculated spectrum of the mixture of conformers and the experimental Raman spectrum of the liquid is reasonably good where the relative intensities of many of the bands are similar to those predicted by the ab initio calculations. As expected, the agreement between the calculated and experimental infrared spectra is also satisfactory. Therefore, these spectra clearly show that calculated spectra can be useful for analytical purposes and contribute significantly to spectral interpretation and vibrational assignments, particularly to distinguish the bands for the individual conformers.

## 4. Vibrational assignment

In order to obtain the conformational stabilities of 4-fluoro-1-pentyne, it is necessary to identify bands for each of the three conformers on the basis of their vibrational assignments. These assignments are based on the ab initio predicted frequencies and group frequencies as well as infrared intensities and Raman activities which were supported by the normal coordinate analysis. All three conformers exist in both fluid and annealed solid phases. However, the intensity of bands belonging to the *F-trans* conformer

Table 1
Calculated and observed vibrational frequencies ($cm^{-1}$) for the *F-trans* conformer of 4-fluoro-1-pentyne

| | Approx. description[a] | HF/6-31G | B3LYP/6-31G(d) | MP2/6-31G(d) unscaled | MP2/6-31G(d) scaled [b] | Gas[c] | Kr sln. | Solid | IR Int[d] | Raman Act[e] | DP ratio | PED |
|---|---|---|---|---|---|---|---|---|---|---|---|---|
| $\nu_1$ | ≡C–H stretch | 3675 | 3495 | 3521 | 3312 | 3330 | 3321 | | 55.2 | 31.4 | 0.20 | $96S_1$ |
| $\nu_2$ | $CH_3$ antisym stretch | 3297 | 3145 | 3220 | 3021 | 2998 | 2995 | | 11.0 | 29.2 | 0.18 | $96S_2$ |
| $\nu_3$ | $CH_3$ antisym stretch | 3294 | 3134 | 3212 | 3013 | 2990 | 2985 | | 17.0 | 68.3 | 0.64 | $95S_3$ |
| $\nu_4$ | $CH_2$ antisym stretch | 3274 | 3084 | 3161 | 2965 | 2958 | 2951 | | 11.5 | 78.5 | 0.56 | $94S_4$ |
| $\nu_5$ | FC–H stretch | 3253 | 3062 | 3128 | 2934 | 2943 | 2940 | | 24.7 | 105.1 | 0.74 | $92S_5$ |
| $\nu_6$ | $CH_3$ sym stretch | 3213 | 3060 | 3118 | 2925 | (2921) | – | | 5.7 | 202.1 | 0.03 | $99S_6$ |
| $\nu_7$ | $CH_2$ sym stretch | 3209 | 3041 | 3104 | 2912 | (2921) | – | | 6.4 | 35.8 | 0.14 | $97S_7$ |
| $\nu_8$ | C ≡ C stretch | 2393 | 2242 | 2169 | 2149 | 2137 | – | | 0.1 | 87.7 | 0.29 | $83S_8$, $14S_{20}$ |
| $\nu_9$ | $CH_3$ antisym def | 1656 | 1529 | 1562 | 1482 | 1464 | 1458 | | 6.0 | 12.6 | 0.70 | $80S_9$, $10S_{11}$ |
| $\nu_{10}$ | $CH_3$ antisym def | 1644 | 1517 | 1551 | 1471 | 1453 | 1449 | | 4.1 | 14.2 | 0.75 | $89S_{10}$ |
| $\nu_{11}$ | $CH_2$ scissor | 1638 | 1502 | 1536 | 1457 | 1441 | 1437 | | 3.2 | 23.6 | 0.73 | $86S_{11}$, $11S_9$ |
| $\nu_{12}$ | $CH_3$ sym def | 1588 | 1443 | 1475 | 1400 | 1390 | 1387 | | 29.2 | 2.4 | 0.51 | $67S_{12}$, $12S_{13}$ |
| $\nu_{13}$ | FC–H bend | 1541 | 1407 | 1438 | 1367 | 1363 | 1360 | | 17.0 | 7.6 | 0.71 | $49S_{13}$, $11S_{12}$ |
| $\nu_{14}$ | FCH def | 1525 | 1403 | 1431 | 1359 | 1348 | 1348 | | 5.0 | 6.7 | 0.46 | $55S_{14}$, $16S_{12}$, $11S_{15}$ |
| $\nu_{15}$ | $CH_2$ wag | 1453 | 1324 | 1338 | 1272 | 1260 | 1257 | | 1.7 | 9.3 | 0.64 | $62S_{15}$, $25S_{14}$ |
| $\nu_{16}$ | $CH_2$ twist | 1389 | 1262 | 1284 | 1222 | 1226 | 1224 | | 6.3 | 4.4 | 0.63 | $55S_{16}$, $15S_{19}$, $10S_{27}$ |
| $\nu_{17}$ | $C_3C_4C_5$ stretch | 1270 | 1162 | 1200 | 1144 | 1139 | 1137 | | 21.3 | 6.3 | 0.75 | $48S_{17}$, $17S_{21}$, $11S_{13}$ |
| $\nu_{18}$ | C–F stretch | 1244 | 1126 | 1152 | 1101 | 1080 | 1081 | 1065 | 46.4 | 1.7 | 0.37 | $37S_{18}$, $17S_{21}$, $15S_{17}$ |
| $\nu_{19}$ | $CH_3$ rock | 1200 | 1119 | 1144 | 1096 | 1060 | 1056 | | 8.0 | 8.0 | 0.62 | $22S_{19}$, $26S_{16}$, $20S_{22}$, $12S_{27}$ |
| $\nu_{20}$ | $C_2$–$C_3$ stretch | 1050 | 984 | 1001 | 955 | 960 | 951 | | 0.8 | 6.9 | 0.73 | $48S_{20}$, $14S_{21}$ |
| $\nu_{21}$ | $CH_3$ rock | 1015 | 954 | 981 | 935 | 932 | 929 | 920 | 37.3 | 2.4 | 0.39 | $22S_{21}$, $35S_{18}$, $19S_{20}$ |
| $\nu_{22}$ | $CH_2$ rock | 1009 | 914 | 930 | 889 | 892 | 889 | | 1.5 | 8.9 | 0.55 | $46S_{22}$, $31S_{19}$ |
| $\nu_{23}$ | $C_3C_4C_5$ stretch | 928 | 853 | 878 | 841 | 838 | 839 | 836 | 2.2 | 9.0 | 0.26 | $49S_{23}$, $15S_{22}$ |
| $\nu_{24}$ | C ≡ C–H bend ip | 907 | 636 | 562 | 632 | 640 | 645 | 665 | 55.7 | 5.5 | 0.35 | $84S_{24}$ |
| $\nu_{25}$ | C ≡ C–H bend op | 896 | 614 | 543 | 614 | 640 | 645 | 665 | 53.1 | 4.9 | 0.69 | $100S_{25}$ |
| $\nu_{26}$ | $C_2C_3C_4$ bend | 574 | 516 | 492 | 504 | 502 | 503 | 503 | 0.7 | 5.0 | 0.48 | $24S_{26}$, $19S_{27}$, $11S_{24}$, $10S_{29}$ |
| $\nu_{27}$ | CFH bend | 498 | 466 | 468 | 460 | 464 | 465 | 466 | 3.1 | 1.6 | 0.22 | $51S_{27}$, $12S_{26}$ |
| $\nu_{28}$ | C–F wag | 433 | 384 | 388 | 382 | 386 | | | 3.3 | 11.8 | 0.74 | $79S_{28}$ |
| $\nu_{29}$ | $C_3C_4C_5$ bend | 397 | 365 | 331 | 367 | 372 | | | 2.3 | 1.6 | 0.60 | $46S_{29}$, $18S_{30}$, $18S_{32}$ |
| $\nu_{30}$ | C ≡ C–C bend op | 370 | 334 | 308 | 334 | 339 | | | 2.6 | 5.0 | 0.75 | $59S_{30}$, $18S_{29}$, $12S_{33}$ |
| $\nu_{31}$ | $CH_3$ torsion | 242 | 243 | 251 | 254 | 231 | | 231 | 0.2 | 0.4 | 0.64 | $91S_{31}$ |
| $\nu_{32}$ | C ≡ C–C bend ip | 171 | 150 | 137 | 149 | 145 | | | 1.1 | 5.7 | 0.73 | $56S_{32}$, $38S_{26}$ |
| $\nu_{33}$ | $C_2C_3C_4F$ torsion | 98 | 92 | 94 | 97 | 88 | | | 1.4 | 3.0 | 0.75 | $85S_{33}$, $11S_{30}$ |

[a] Abbreviations: antisym, antisymmetric; sym, symmetric; def, deformation; ip, in-plane (C ≡ CCF plane) and op: out-of-plane.

[b] Force constant scaling factors: 0.9 for heavy atom stretching except 1.0 for C ≡ C, 0.88 for CH stretching; 1.0 for heavy atom bending except 1.5 for C ≡ C–C bending; 0.9 for CH bending except 1.3 for C ≡ C–H; and 1.0 for torsion.

[c] Values in parenthesis come from Raman spectrum of liquid.

[d] Infrared intensities in km/mol and PED taken from MP2/6-31G(d) unscaled.

[e] Raman activities in $Å^4$/amu and DP ratios from HF/6-31G(d).

Table 2
Calculated and observed vibrational frequencies ($cm^{-1}$) for the *H-trans* conformer of 4-fluoro-1-pentyne

| | Approx. description[a] | HF/6-31G | B3LYP/6-31G(d) | MP2/6-31G(d) unscaled | MP2/6-31G(d) scaled[b] | Gas | Kr sln. | Solid | IR Int[c] | Raman Act[d] | DP ratio | PED |
|---|---|---|---|---|---|---|---|---|---|---|---|---|
| $\nu_1$ | ≡C–H stretch | 3676 | 3496 | 3522 | 3313 | | | 3288 | 52.7 | 31.8 | 0.20 | $96S_1$ |
| $\nu_2$ | $CH_3$ antisym stretch | 3307 | 3149 | 3226 | 3026 | 3002 | | | 11.3 | 33.2 | 0.61 | $94S_3$ |
| $\nu_3$ | $CH_3$ antisym stretch | 3282 | 3133 | 3210 | 3011 | | | 2986 | 13.9 | 74.9 | 0.71 | $94S_3$ |
| $\nu_4$ | $CH_2$ antisym stretch | 3259 | 3078 | 3154 | 2958 | | | 2963 | 6.9 | 165.6 | 0.24 | $98S_4$ |
| $\nu_5$ | FC–H stretch | 3248 | 3064 | 3119 | 2926 | 2950 | 2940 | | 11.9 | 76.3 | 0.73 | $89S_6$ |
| $\nu_6$ | $CH_3$ sym stretch | 3209 | 3049 | 3112 | 2920 | 2937 | 2928 | 2940 | 48.1 | 135.1 | 0.03 | $76S_5$, $13S_7$ |
| $\nu_7$ | $CH_2$ sym stretch | 3200 | 3035 | 3098 | 2906 | | | 2877 | 2.1 | 61.9 | 0.17 | $83S_7$, $15S_5$ |
| $\nu_8$ | C ≡ C stretch | 2395 | 2243 | 2169 | 2149 | | | 2125 | 0.1 | 84.0 | 0.29 | $83S_8$, $14S_{20}$ |
| $\nu_9$ | $CH_3$ antisym def | 1657 | 1529 | 1563 | 1483 | 1471 | 1465 | 1460 | 4.9 | 13.8 | 0.72 | $89S_9$ |
| $\nu_{10}$ | $CH_3$ antisym def | 1642 | 1515 | 1549 | 1469 | | | 1449 | 2.9 | 16.0 | 0.73 | $87S_{10}$ |
| $\nu_{11}$ | $CH_2$ scissor | 1629 | 1491 | 1525 | 1447 | 1424 | 1419 | 1417 | 6.1 | 19.9 | 0.72 | $94S_{11}$ |
| $\nu_{12}$ | $CH_3$ sym def | 1590 | 1446 | 1478 | 1402 | | | 1389 | 28.6 | 2.6 | 0.51 | $67S_{12}$, $13S_{13}$ |
| $\nu_{13}$ | FC–H wag | 1556 | 1406 | 1432 | 1359 | | | 1344 | 5.8 | 5.3 | 0.70 | $27S_{13}$, $31S_{14}$, $25S_{12}$ |
| $\nu_{14}$ | FCH bend | 1517 | 1404 | 1430 | 1359 | | | 1344 | 16.2 | 4.0 | 0.72 | $42S_{14}$, $25S_{13}$, $18S_{15}$ |
| $\nu_{15}$ | $CH_2$ wag | 1482 | 1349 | 1382 | 1316 | 1310 | 1309 | 1310 | 16.5 | 8.3 | 0.30 | $54S_{15}$, $17S_{17}$ |
| $\nu_{16}$ | $CH_2$ twist | 1395 | 1272 | 1289 | 1226 | 1234 | 1231 | 1230 | 4.1 | 13.7 | 0.75 | $68S_{16}$ |
| $\nu_{17}$ | $C_3C_4C_5$ stretch | 1282 | 1178 | 1210 | 1156 | | | 1139 | 15.7 | 6.6 | 0.72 | $26S_{17}$, $18S_{19}$, $14S_{21}$ |
| $\nu_{18}$ | C–F stretch | 1239 | 1126 | 1150 | 1100 | | 1089 | 1085 | 23.6 | 1.8 | 0.75 | $15S_{18}$, $15S_{16}$, $15S_{21}$,$15S_{22}$ |
| $\nu_{19}$ | $CH_3$ rock | 1183 | 1085 | 1109 | 1057 | | | 1050 | 15.8 | 3.9 | 0.72 | $18S_{19}$, $14S_{17}$, $12S_{18}$ |
| $\nu_{20}$ | $C_2$–$C_3$ stretch | 1059 | 978 | 1005 | 955 | | | | 17.6 | 8.2 | 0.75 | $37S_{21}$, $24S_{18}$, $15S_{20}$,$13S_{23}$ |
| $\nu_{21}$ | $CH_3$ rock | 1008 | 925 | 945 | 903 | 904 | 903 | 900 | 4.7 | 6.1 | 0.74 | $32S_{20}$, $19S_{19}$, $13S_{17}$ |
| $\nu_{22}$ | $CH_2$ rock | 982 | 907 | 928 | 891 | | | 878 | 8.8 | 7.3 | 0.64 | $61S_{22}$, $21S_{19}$ |
| $\nu_{23}$ | $C_3C_4C_5$ stretch | 902 | 805 | 834 | 801 | | 797 | 796 | 8.8 | 5.7 | 0.67 | $22S_{23}$, $39S_{17}$, $16S_{18}$ |
| $\nu_{24}$ | $C_2C_3C_4$ bend | 884 | 665 | 673 | 676 | 640 | 645 | 665 | 13.2 | 4.1 | 0.75 | $26S_{26}$, $27S_{27}$, $11S_{20}$,$11S_{19}$ |
| $\nu_{25}$ | C ≡ C–H bend ip | 852 | 625 | 537 | 598 | 640 | 645 | 665 | 44.4 | 13.7 | 0.06 | $97S_{24}$ |
| $\nu_{26}$ | C ≡ C–H bend op | 723 | 604 | 528 | 592 | | | | 51.5 | 1.6 | 0.41 | $100S_{25}$ |
| $\nu_{27}$ | CFH bend | 468 | 433 | 429 | 429 | 430 | 432 | 434 | 4.4 | 3.3 | 0.71 | $56S_{28}$, $19S_{27}$ |
| $\nu_{28}$ | C–F wag | 418 | 374 | 365 | 366 | 387 | | 376 | 2.0 | 9.9 | 0.75 | $45S_{29}$, $13S_{28}$ |
| $\nu_{29}$ | $C_3C_4C_5$ bend | 394 | 351 | 334 | 351 | 347 | | 346 | 0.4 | 6.0 | 0.75 | $32S_{29}$, $24S_{32}$, $12S_{26}$,$11S_{27}$ |
| $\nu_{30}$ | C ≡ C–C bend op | 364 | 330 | 288 | 325 | 333 | | 332 | 0.8 | 1.9 | 0.74 | $61S_{30}$, $15S_{31}$, $14S_{33}$ |
| $\nu_{31}$ | $CH_3$ torsion | 242 | 242 | 252 | 256 | 231 | | | 0.1 | 0.1 | 0.50 | $82S_{31}$, $16S_{30}$ |
| $\nu_{32}$ | C ≡ C–C bend ip | 174 | 152 | 139 | 153 | 148 | | | 0.1 | 5.3 | 0.72 | $58S_{32}$, $35S_{26}$ |
| $\nu_{33}$ | $C_2C_3C_4F$ torsion | 95 | 87 | 91 | 93 | 89 | | 111 | 1.6 | 2.7 | 0.75 | $79S_{33}$, $16S_{30}$ |

[a] Abbreviations: antisym, antisymmetric; sym, symmetric; def, deformation; ip, in-plane (C ≡ CCH plane) and op: out-of-plane.

[b] Force constant scaling factors: 0.9 for heavy atom stretching except 1.0 for C ≡ C, 0.88 for CH stretching; 1.0 for heavy atom bending except 1.5 for C ≡ C–C bending; 0.9 for CH bending except 1.3 for C ≡ C–H; and 1.0 for torsion.

[c] Infrared intensities in km/mol and PED taken from MP2/6-31G(d) unscaled.

[d] Raman activities in $Å^4$/amu and DP ratios from HF/6-31G(d).

Table 3
Calculated and observed vibrational frequencies ($cm^{-1}$) for the *Me-trans* conformer of 4-fluoro-1-pentyne

| | Approx. description[a] | HF/6-31G | B3LYP/6-31G(d) | MP2/6-31G(d) unscaled | MP2/6-31G(d) scaled[b] | Gas | Kr sln. | Solid | IR Int[c] | Raman Act[d] | DP ratio | PED |
|---|---|---|---|---|---|---|---|---|---|---|---|---|
| $\nu_1$ | ≡C–H stretch | 3676 | 3496 | 3523 | 3313 | | | | 53.9 | 31.9 | 0.20 | $96S_1$ |
| $\nu_2$ | $CH_3$ antisym stretch | 3298 | 3139 | 3216 | 3017 | | | | 13.4 | 45.7 | 0.27 | $60S_2$, $39S_3$ |
| $\nu_3$ | $CH_3$ antisym stretch | 3287 | 3130 | 3209 | 3010 | | | | 17.5 | 67.0 | 0.73 | $60S_3$, $39S_2$ |
| $\nu_4$ | $CH_2$ antisym stretch | 3271 | 3077 | 3152 | 2957 | | | | 12.3 | 87.2 | 0.60 | $91S_4$ |
| $\nu_5$ | FC–H stretch | 3243 | 3059 | 3126 | 2933 | | | | 20.9 | 83.7 | 0.64 | $90S_5$ |
| $\nu_6$ | $CH_3$ sym stretch | 3206 | 3058 | 3115 | 2922 | | | | 8.7 | 201.3 | 0.01 | $99S_6$ |
| $\nu_7$ | $CH_2$ sym stretch | 3199 | 3036 | 3097 | 2905 | | | | 8.9 | 21.4 | 0.29 | $98S_7$ |
| $\nu_8$ | C ≡ C stretch | 2397 | 2246 | 2172 | 2152 | | | 2125 | 0.1 | 95.2 | 0.30 | $83S_8$, $14S_{20}$ |
| $\nu_9$ | $CH_3$ antisym def | 1655 | 1529 | 1561 | 1481 | | | | 4.5 | 19.2 | 0.75 | $89S_9$ |
| $\nu_{10}$ | $CH_3$ antisym def | 1643 | 1516 | 1549 | 1470 | | | | 4.4 | 23.0 | 0.75 | $87S_{10}$ |
| $\nu_{11}$ | $CH_2$ scissor | 1625 | 1488 | 1522 | 1445 | | | | 3.2 | 5.9 | 0.67 | $95S_{11}$ |
| $\nu_{12}$ | $CH_3$ sym def | 1587 | 1441 | 1472 | 1397 | | | | 19.0 | 1.6 | 0.66 | $73S_{12}$ |
| $\nu_{13}$ | FC–H wag | 1549 | 1412 | 1445 | 1373 | 1369 | 1366 | 1368 | 14.0 | 8.2 | 0.60 | $41S_{13}$, $21S_{15}$, $14S_{12}$ |
| $\nu_{14}$ | FCH bend | 1513 | 1407 | 1432 | 1360 | | | 1357 | 11.3 | 8.6 | 0.72 | $72S_{14}$ |
| $\nu_{15}$ | $CH_2$ wag | 1475 | 1332 | 1352 | 1286 | 1288 | 1291 | 1288 | 5.1 | 7.8 | 0.59 | $56S_{15}$, $27S_{13}$ |
| $\nu_{16}$ | $CH_2$ twist | 1385 | 1267 | 1287 | 1224 | | | | 3.7 | 7.9 | 0.66 | $70S_{16}$ |
| $\nu_{17}$ | $C_3C_4C_5$ stretch | 1273 | 1167 | 1202 | 1147 | 1140 | | 1133 | 33.3 | 5.7 | 0.62 | $22S_{17}$, $29S_{21}$, $17S_{18}$ |
| $\nu_{19}$ | $CH_3$ rock | 1247 | 1138 | 1166 | 1117 | | 1118 | 1113 | 7.7 | 5.7 | 0.28 | $30S_{19}$, $29S_{23}$, $12S_{27}$ |
| $\nu_{18}$ | C–F stretch | 1189 | 1100 | 1130 | 1076 | | | 1055 | 31.4 | 7.4 | 0.69 | $24S_{18}$, $21S_{17}$, $20S_{22}$, $11S_{16}$ |
| $\nu_{20}$ | $C_2$–$C_3$ stretch | 1073 | 998 | 1020 | 973 | | 976 | 972 | 8.3 | 5.3 | 0.75 | $42S_{20}$, $16S_{21}$, $11S_{17}$ |
| $\nu_{21}$ | $CH_3$ rock | 1017 | 930 | 954 | 909 | | | | 6.0 | 5.7 | 0.74 | $32S_{21}$, $19S_{17}$, $18S_{20}$, $16S_{18}$ |
| $\nu_{22}$ | $CH_2$ rock | 987 | 910 | 926 | 888 | | 881 | | 3.9 | 7.7 | 0.54 | $44S_{22}$, $21S_{19}$ |
| $\nu_{23}$ | $C_3C_4C_5$ stretch | 909 | 845 | 867 | 834 | 826 | 828 | 820 | 15.7 | 10.2 | 0.38 | $32S_{23}$, $25S_{18}$, $13S_{19}$ |
| $\nu_{24}$ | C ≡ C–H bend ip | 894 | 623 | 565 | 622 | | | | 48.6 | 4.3 | 0.23 | $48S_{24}$, $14S_{26}$, $12S_{32}$ |
| $\nu_{25}$ | C ≡ C–H bend op | 883 | 601 | 524 | 592 | | | | 50.5 | 4.9 | 0.63 | $97S_{25}$ |
| $\nu_{26}$ | $C_2C_3C_4$ bend | 593 | 540 | 501 | 515 | 531 | 533 | 533 | 14.1 | 6.3 | 0.35 | $17S_{26}$, $45S_{24}$, $17S_{28}$ |
| $\nu_{27}$ | CFH bend | 495 | 464 | 467 | 454 | 464 | 465 | 466 | 0.8 | 1.4 | 0.29 | $63S_{27}$, $10S_{22}$ |
| $\nu_{28}$ | C–F wag | 410 | 371 | 366 | 365 | | | 376 | 3.3 | 12.3 | 0.75 | $51S_{28}$, $18S_{29}$ |
| $\nu_{29}$ | $C_3C_4C_5$ bend | 395 | 349 | 313 | 328 | | | | 0.5 | 3.1 | 0.72 | $57S_{29}$, $24S_{32}$ |
| $\nu_{30}$ | C ≡ C–C bend op | 359 | 326 | 277 | 323 | | | | 0.4 | 3.3 | 0.62 | $75S_{30}$, $15S_{33}$ |
| $\nu_{31}$ | $CH_3$ torsion | 235 | 233 | 244 | 245 | | | | 0.1 | 0.1 | 0.75 | $94S_{31}$ |
| $\nu_{32}$ | C ≡ C–C bend ip | 167 | 146 | 130 | 143 | 137 | | | 0.2 | 5.8 | 0.74 | $56S_{32}$, $35S_{26}$ |
| $\nu_{33}$ | $C_2C_3C_4F$ torsion | 89 | 84 | 88 | 90 | 86 | | | 0.7 | 2.9 | 0.75 | $84S_{33}$, $15S_{30}$ |

[a] Abbreviations: antisym, antisymmetric; sym, symmetric; def, deformation; ip, in-plane (C ≡ CCC plane) and op: out-of-plane.

[b] Force constant scaling factors: 0.9 for heavy atom stretching except 1.0 for C ≡ C, 0.88 for CH stretching; 1.0 for heavy atom bending except 1.5 for C ≡ C–C bending; 0.9 for CH bending except 1.3 for C ≡ C–H; and 1.0 for torsion.

[c] Infrared intensities in km/mol and PED taken from MP2/6-31G(d) unscaled.

[d] Raman activities in $Å^4$/amu and DP ratios from HF/6-31G(d).

Table 4
Calculated energies and energy difference for several conformations of 4-fluoro-1-pentyne by ab initio and hybrid DFT methods

| Method/basis | Energy ($E_h$) | Energy differences[a] ($cm^{-1}$) | |
|---|---|---|---|
| | *F-trans* | *H-trans* | *Me-trans* |
| HF/6-31G | −292.692524 | 637 | 641 |
| $C_2C_3C_4F$ dihedral | *−174.0* | *65.6* | *−64.9* |
| MP2(full)/6-31G(d) | −293.595502 | 269 | 428 |
| $C_2C_3C_4F$ dihedral | *−176.0* | *64.2* | *−61.4* |
| MP2(full)/6-311 + G(d,p) | −293. 790849 | 253 | 458 |
| $C_2C_3C_4F$ dihedral | *−175.8* | *67.0* | *−63.3* |
| MP2(full)/6-311 + G(2d,2p) | −293.861262 | 297 | 438 |
| $C_2C_3C_4F$ dihedral | *−174.5* | *66.8* | *−63.7* |
| B3LYP/6-31G(d) | −294.514210 | 387 | 398 |
| $C_2C_3C_4F$ dihedral | *−174.5* | *65.7* | *−62.3* |
| B3LYP/6-311 + G(2d,2p) | −294.623000 | 321 | 359 |
| $C_2C_3C_4F$ dihedral | *−172.6* | *67.9* | *−65.1* |
| MP2/DZ(d) | −293.636263 | 327 | 427 |
| $C_2C_3C_4F$ dihedral | *−173.4* | *65.8* | *−62.8* |
| B3LYP/DZ(d) | −294.566615 | 405 | 392 |
| B3LYP/DZ(d,p) | −294.577040 | 401 | 377 |
| B3LYP/cc-pVDZ | −294.530855 | 467 | 420 |
| B3LYP/cc-pVTZ | −294.636080 | 337 | 401 |

The molecule is chiral and calculations were made for the R configuration.
[a] Energies of conformations relative to *F-trans*.

was found to decrease significantly in the spectra of the annealed solid whereas the intensities of the other conformer bands slightly increased. Therefore, most of the pronounced peaks in the spectra of the annealed solid phase were assigned to the two conformers of lesser abundance in the fluid phases. However, it should be noted that the *F-trans* conformer is predicted as the most stable conformer from the ab initio calculations. Thus, a larger number of the bands in the spectra of the fluid phases are assigned to the fundamental modes of the *F-trans* conformer and for those bands which increased in intensity upon crystallization were assigned to the *H-trans* and *Me-trans* conformers.

For the *F-trans* conformer, a total of seven carbon–hydrogen stretching modes are expected and the highest one is the ≡CH stretch ($\nu_1$) which is observed at 3330 $cm^{-1}$. There are seven distinct Q-branches with strong absorptions observed in the range from 2900 to 3010 $cm^{-1}$. Four of them can be assigned to the fundamental modes of the *F-trans* conformer ($\nu_2-\nu_5$). However, the peaks at 2950 and 2937 $cm^{-1}$ are assigned to the $CH_3$ antisymmetric and symmetric stretches of the *H-trans* conformer ($\nu_2'-\nu_5'$), respectively with the predicted intensities of 17.0 and 48.1 km/mol. By using the 'group frequencies' for the $CH_2$ scissor, wag, twist and rock ($\nu_{11}$, $\nu_{15}$, $\nu_{16}$ and $\nu_{22}$), these fundamentals can be easily assigned to the infrared bands at 1441, 1260, 1226 and 892 $cm^{-1}$, respectively. The ≡CH bends, with the predicted infrared intensities of 55.7 and 53.1 km/mol respectively for in-plane and out-of-plane modes, must to assign to two infrared bands at 645 and 632 $cm^{-1}$ with strong absorption in the spectrum of krypton solution. For these fundamentals, two scaling factor of 1.3 and 1.5 were used since they are predicted too high at the RHF level but too low at MP2 level. It should be noted that the B3LYP/6-31G(d) calculation gives a much better predicted frequencies for these modes.

The predicted contours of $C_3C_4C_5$ stretches ($\nu_{17}$, $\nu_{23}$) for the *F-trans* conformer are almost pure A-types. Therefore, these two fundamental modes are assigned to the two A-type bands at 1139 and 838 $cm^{-1}$, respectively. The C ≡ C stretch is confidently assigned to the Raman band at 2125 $cm^{-1}$. The C ≡ CC in-plane and out-of-plane bends are assigned to the infrared bands at 145 and 339 $cm^{-1}$, respectively, which are consistent with the ab initio predictions at the MP2 level with proper scaling factors. The $C_2C_3C_4$ bends ($\nu_{26}$, $\nu_{26}''$) are expected at 504 and 515 $cm^{-1}$, respectively, for the *F-trans* and *Me-trans* conformers. Therefore, the two peaks at 502 and 531 $cm^{-1}$ in the infrared spectrum of krypton solution are assigned to these two modes with the intensity of the first band decreased significantly in the spectrum of the annealed solid. The most challenging assignments are for the bands between 1000 and 1100 $cm^{-1}$ (Fig. 7). Ab initio calculations predicted that a total of six fundamental modes existing for the three conformers in this region. The infrared band at 1065 $cm^{-1}$ in the spectrum of the annealed solid is assigned to the CF stretch for the *F-trans* conformer ($\nu_{18}$) because its intensity decreased significantly after annealing. However, this fundamental has to be assigned to the band at 1081 $cm^{-1}$ in the spectrum of the krypton solution. Two strong bands at 1055 and 1050 $cm^{-1}$ in the spectrum of the solid can be assigned to the $\nu_{18}''$ and $\nu_{19}'$ fundamentals (*Me-trans* and *H-trans*), respectively, in agreement with the ab

Table 5
Geometrical parameters for the three stable conformers of 4-fluoro-1-pentyne calculated *by ab initio* and B3LYP methods

| | | Ts form (*F-trans*) | | | Gs form (*H-trans*) | | | –Gs form (*Me-trans*) | | |
|---|---|---|---|---|---|---|---|---|---|---|
| | | HF/6-31G | MP2 /6-31G(d) | B3LYP/6-31G(d) | HF/6-31G | MP2/6-31G(d) | B3LYP/6-31G(d) | HF/6-31G | MP2/6-31G(d) | B3LYP/6-31G(d) |
| $C_1 \equiv C_2$ | $S$ | 1.1949 | 1.2205 | 1.2075 | 1.1945 | 1.2203 | 1.2072 | 1.1942 | 1.2200 | 1.2069 |
| $C_2-C_3$ | $T$ | 1.4652 | 1.4623 | 1.4614 | 1.4650 | 1.4633 | 1.4631 | 1.4646 | 1.4627 | 1.4622 |
| $C_3-C_4$ | $U$ | 1.5265 | 1.5264 | 1.5380 | 1.5254 | 1.5262 | 1.5383 | 1.5237 | 1.5242 | 1.5357 |
| $C_4-C_5$ | $V$ | 1.5111 | 1.5108 | 1.5177 | 1.5114 | 1.5113 | 1.5186 | 1.5133 | 1.5131 | 1.5200 |
| $C_4-F$ | $X$ | 1.4314 | 1.4073 | 1.4008 | 1.4279 | 1.4041 | 1.3979 | 1.4279 | 1.4037 | 1.3973 |
| $C_2C_3C_4$ | $\theta$ | 112.8 | 112.2 | 113.3 | 114.4 | 113.0 | 114.3 | 113.5 | 112.5 | 113.5 |
| $C_3C_4C_5$ | $\varepsilon$ | 115.2 | 114.0 | 114.3 | 115.7 | 114.4 | 114.8 | 113.6 | 113.2 | 113.0 |
| $C_1H_1$ | $r_1$ | 1.053 | 1.0666 | 1.0663 | 1.0529 | 1.0665 | 1.0663 | 1.0529 | 1.0664 | 1.0662 |
| $C_3H_2$ | $r_2$ | 1.0838 | 1.0956 | 1.0975 | 1.0857 | 1.0974 | 1.0990 | 1.0844 | 1.0966 | 1.0985 |
| $C_3H_3$ | $r_3$ | 1.0844 | 1.0965 | 1.0985 | 1.0839 | 1.0959 | 1.0975 | 1.0854 | 1.0971 | 1.0988 |
| $C_4H_4$ | $r_4$ | 1.0790 | 1.0957 | 1.0971 | 1.0806 | 1.0972 | 1.0984 | 1.0787 | 1.0957 | 1.0972 |
| $C_5H_5$ | $r_5$ | 1.0819 | 1.0923 | 1.0943 | 1.0818 | 1.0923 | 1.0943 | 1.0816 | 1.0922 | 1.0942 |
| $C_5H_6$ | $r_6$ | 1.0819 | 1.0924 | 1.0943 | 1.0836 | 1.0939 | 1.0958 | 1.0834 | 1.0935 | 1.0955 |
| $C_5H_7$ | $r_7$ | 1.0828 | 1.0934 | 1.0958 | 1.0808 | 1.0917 | 1.0938 | 1.0829 | 1.093 | 1.0956 |
| $C_3C_4F$ | $\gamma_8$ | 105.5 | 106.4 | 106.5 | 107.6 | 107.7 | 108.1 | 107.5 | 107.6 | 108.1 |
| $C_2C_3H_2$ | $\gamma_2$ | 109.8 | 110.4 | 110.1 | 109.5 | 110.1 | 109.8 | 109.7 | 110.1 | 110.0 |
| $C_2C_3H_3$ | $\gamma_3$ | 110.1 | 110.5 | 110.3 | 109.3 | 109.8 | 109.7 | 109.4 | 110.1 | 109.8 |
| $C_3C_4H_4$ | $\gamma_4$ | 110.5 | 109.8 | 109.4 | 108.8 | 108.7 | 107.8 | 110.7 | 109.9 | 109.5 |
| $C_4C_5H_5$ | $\beta_5$ | 110.2 | 110.1 | 110.2 | 110.0 | 109.8 | 109.9 | 110.0 | 109.9 | 109.9 |
| $C_4C_5H_6$ | $\beta_6$ | 110.6 | 110.5 | 110.4 | 110.5 | 110.6 | 110.6 | 110.7 | 110.9 | 111.0 |
| $C_4C_5H_7$ | $\beta_7$ | 110.4 | 109.7 | 110.3 | 110.6 | 109.8 | 110.3 | 110.6 | 109.9 | 110.5 |
| $C_5C_3C_4F$ | | 118.5 | 119.3 | 120.0 | 120.5 | 120.3 | 121.4 | 118.6 | 119.2 | 119.9 |
| $C_4C_2C_3H_2$ | | −120.7 | −120.9 | −120.9 | −121.7 | −121.6 | −121.9 | −121.4 | −120.5 | −121.2 |
| $C_4C_2C_3H_3$ | | 121.7 | 120.8 | 121.6 | 121.4 | 120.8 | 121.3 | 121.5 | 121.7 | 121.7 |
| $C_5C_3C_4H_4$ | | −127.6 | −125.3 | −124.6 | −125.7 | −124.4 | −123.5 | −126.4 | −124.8 | −123.9 |
| $C_3C_4C_5H_5$ | $\tau_1$ | 175.8 | 176.9 | 177.7 | 178.8 | 178.4 | 178.1 | 175.0 | 176.2 | 176.2 |
| $H_5C_4C_5H_6$ | | 120.1 | 120.5 | 120.3 | 119.8 | 120.0 | 119.8 | 119.9 | 120.2 | 119.9 |
| $H_5C_4C_5H_7$ | | −119.6 | −119.5 | −119.7 | −119.9 | −119.8 | -120.0 | -119.5 | -119.4 | -119.5 |
| $C_2C_3C_4C_5$ | $\tau_2$ | 67.5 | 64.8 | 65.6 | −54.9 | −56.0 | −55.7 | 176.5 | −180.6 | 177.9 |
| $C_2C_3C_4F$ | | −174.0 | −176.0 | −174.5 | 65.6 | 64.2 | 65.7 | −64.9 | −61.4 | −62.3 |
| | $\lvert\mu_a\rvert$ | 1.729 | 1.347 | 0.935 | 0.112 | 0.196 | 0.195 | 0.682 | 0.719 | 0.709 |
| | $\lvert\mu_b\rvert$ | 1.247 | 0.916 | 0.773 | 1.307 | 0.933 | 0.786 | 2.502 | 1.951 | 1.647 |
| | $\lvert\mu_c\rvert$ | 0.247 | 0.205 | 0.122 | 2.284 | 1.850 | 1.536 | 0.809 | 0.658 | 0.494 |
| | $\lvert\mu_T\rvert$ | 2.146 | 1.642 | 1.219 | 2.634 | 2.081 | 1.736 | 2.717 | 2.180 | 1.861 |
| | $a_0$ | | 3.90 | | | 3.80 | | | 4.06 | |
| | $A$ | 7708 | 7760 | 7686 | 5619 | 5593 | 5632 | 8099 | 8202 | 8164 |
| | $B$ | 2038 | 2052 | 2036 | 2378 | 2409 | 2361 | 2064 | 2081 | 2058 |
| | $C$ | 1716 | 1728 | 1714 | 2220 | 2261 | 2204 | 1758 | 1770 | 1752 |
| | $\kappa$ | | | -0.8921 | | | -0.9083 | | | -0.8998 |
| | $I_\tau$ | | | 3.1874 | | | 3.1875 | | | 3.1241 |
| | $F$ | | | 5.3578 | | | 5.3694 | | | 5.6435 |

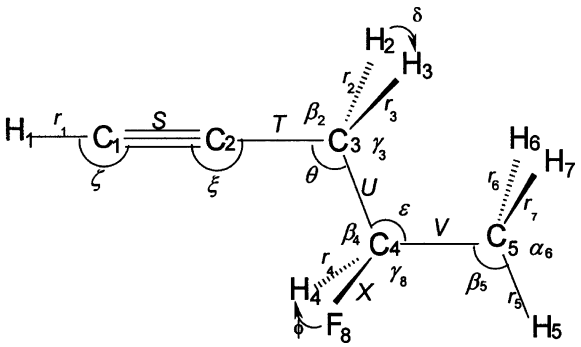


Fig. 5. Internal coordinates for 4-fluoro-1-pentyne.

initio calculations. The predicted frequencies of the asymmetric torsion for all three conformers are lower than 100 $cm^{-1}$. Therefore, the infrared peaks at 87.8, 88.6 and 85.7 $cm^{-1}$ are assigned as the $1 \leftarrow 0$ transitions of the *F-trans*, *H-trans* and *Me-trans* conformers, respectively (Fig. 8). The complete assignments for the observed fundamentals of 4-fluoro-1-pentyne are reported in Tables 1–3.

## 5. Conformational stability

For 4-fluoro-1-pentyne, there are three stable conformers according to the ab initio predictions. The determination of the enthalpy differences among three conformers is rather difficult because most of the conformer bands are near coincident. Nevertheless, some of the conformer bands can be identified by carefully comparing the spectra of the sample in the fluid states with the corresponding spectra of the annealed solid. The intensities of the infrared bands at 1257, 951, 839 and 502 $cm^{-1}$ in the spectra of krypton solution and Raman lines at 1091, 1069, 958, 921, 857, 503 and 389 $cm^{-1}$ in the spectrum of the liquid decreased significantly in the spectrum of the annealed solid. All of these peaks are predicted as the fundamentals of the *F-trans* conformer which is supported by the ab initio calculations. For example, the peak at 503 $cm^{-1}$ in both infrared spectrum of krypton solution and Raman spectrum of liquid which is a key in the determination of the conformational stability, is confidently assigned to the fundamental of the *F-trans* conformer with a predicted value of 504 $cm^{-1}$ from the MP2/6-31G(d) calculations. For the *H-trans* and *Me-trans* conformers, the bands at 533 and 432 $cm^{-1}$ with increased intensities in the spectrum of the solid (Fig. 4) are assigned to these conformers, respectively, and are therefore used for the conformational stability determinations. Additionally, the 839 $cm^{-1}$ band of the *F-trans* conformer, the 1031 $cm^{-1}$ band of the *H-trans*

Table 6
Symmetry coordinates for vibrations of 4-fluoro-1-pentyne

| Description | Symmetry coordinate |
|---|---|
| ≡C–H stretch | $S_1 = r_1$ |
| $CH_3$ antisymmetric stretch | $S_2 = r_5 - r_6$ |
| $CH_3$ antisymmetric stretch | $S_3 = 2r_7 - r_5 - r_6$ |
| $CH_2$ antisymmetric stretch | $S_4 = r_2 - r_3$ |
| FC–H stretch | $S_5 = r_4$ |
| $CH_3$ symmetric stretch | $S_6 = r_5 + r_6 + r_7$ |
| $CH_2$ symmetric stretch | $S_7 = r_2 + r_3$ |
| C ≡ C stretch | $S_8 = S$ |
| $CH_3$ antisymmetric deformation | $S_9 = 2\alpha_6 - \alpha_5 - \alpha_7$ |
| $CH_3$ antisymmetric deformation | $S_{10} = \alpha_5 - \alpha_7$ |
| $CH_2$ scissors | $S_{11} = (\sqrt{6}+2)\delta - \beta_2 - \beta_3 - \gamma_2 - \gamma_3 - (\sqrt{6}-2)\theta$ |
| $CH_3$ symmetric deformation | $S_{12} = \alpha_5 + \alpha_6 + \alpha_7 - \beta_5 - \beta_6 - \beta_7$ |
| FC–H bend | $S_{13} = \beta_4 - \gamma_4$ |
| FCH deformation | $S_{14} = 2\phi - \beta_4 - \gamma_4$ |
| $CH_2$ wag | $S_{15} = \beta_6 + \beta_7 - \gamma_6 - \gamma_7$ |
| $CH_2$ twist | $S_{16} = \beta_6 - \beta_7 - \gamma_6 + \gamma_7$ |
| $C_3C_4$ and $C_4C_5$ stretch combination | $S_{17} = U - V$ |
| C–F stretch | $S_{18} = X$ |
| $CH_3$ rock | $S_{19} = 2\beta_7 - \beta_5 - \beta_6$ |
| $C_2$–$C_3$ stretch | $S_{20} = T$ |
| $CH_3$ rock | $S_{21} = \beta_5 - \beta_6$ |
| $CH_2$ rock | $S_{22} = \beta_2 - \beta_3 + \gamma_2 - \gamma_3$ |
| $C_3C_4$ and $C_4C_5$ stretch combination | $S_{23} = U + V$ |
| C ≡ C–H bend ip | $S_{24} = \zeta$ |
| C ≡ C–H bend op | $S_{25} = \zeta'$ |
| $C_2C_3C_4$ bend | $S_{26} = (\sqrt{6}+2)\theta - \beta_2 - \beta_3 - \gamma_2 - \gamma_3 - (\sqrt{6}-2)\delta$ |
| FC–H bend | $S_{27} = \varepsilon + \beta_8 + \gamma_8 - \phi - \beta_4 - \gamma_4$ |
| C–F wag | $S_{28} = \beta_8 - \gamma_8$ |
| $C_3C_4C_5$ bend | $S_{29} = 2\varepsilon - \beta_8 - \gamma_8$ |
| C ≡ C–C bend op | $S_{30} = \xi'$ |
| $CH_3$ torsion | $S_{31} = \tau_1$ |
| C ≡ C–C bend ip | $S_{32} = \xi$ |
| $C_2C_3C_4F$ torsion | $S_{33} = \tau_2$ |
| $CH_3$ redundancy | $R_1 = \alpha_5 + \alpha_6 + \alpha_7 + \beta_5 + \beta_6 + \beta_7$ |
| $CH_2$ redundancy | $R_2 = \theta + \beta_2 + \beta_3 + \gamma_2 + \gamma_3 + \delta$ |
| CHF redundancy | $R_3 = \varepsilon + \beta_4 + \beta_8 + \gamma_4 + \gamma_8 + \phi$ |

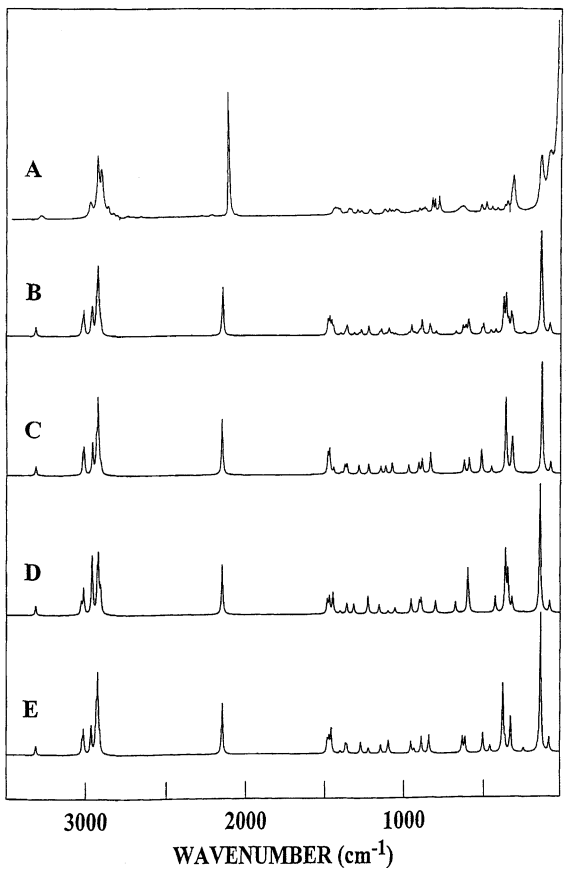


Fig. 6. Raman spectra of 4-fluoro-1-pentyne: (A) liquid state; (B) simulated Raman spectrum of the *F-trans*, *H-trans* and *Me-trans* conformers mixture with a $\Delta H$ 129 and 178 $cm^{-1}$; (C) calculated for the pure *Me-trans* conformer; (D) calculated for the pure *H-trans* conformer; and (E) calculated for the pure *F-trans* conformer.

conformer, and the 827 and 1291 $cm^{-1}$ bands of the *Me-trans* conformer were clearly identified as arising from these indicated rotamers.

In order to obtain the enthalpy differences among the three conformers, the temperature dependent infrared spectra of sample dissolved in the liquid krypton with the temperature range from −105 to −135 °C were recorded. The spectra shown in Fig. 9 clearly demonstrate that the intensities of the *F-trans* band at 503 $cm^{-1}$ increases whereas the intensities of the bands due to the *H-trans* and *Me-trans* conformers at 533 and 432 $cm^{-1}$, respectively, decrease with lowering the temperature which is in agreement with the theoretical predictions of the stabilities. Six conformer pairs were utilized in the enthalpy difference determination. The intensities of these conformer pairs were used to fit van't Hoff equation $\ln K = \Delta H/RT - \Delta S/R$ with the assumption that the value of $\Delta H$ is not the function of temperature within the experimental temperature range. By fitting the slope of the lines with least square fit, the enthalpy difference between the *F-trans* and *Me-trans* conformers is 178 ± 10 $cm^{-1}$ (2.13 ± 0.12 kJ/mol) with the *F-trans* conformer the more stable form whereas the difference is 129 ± 9 $cm^{-1}$ (1.54 ± 0.11 kJ/mol) between the *F-trans* and *H-trans* conformers again with the *F-trans* form the more stable conformer (Table 7). Because of the possible contributions to the intensities from overtones and combination bands which may be nearly coincident to these fundamentals, the experimental uncertainness should be at least ten percent. Thus,

Table 7
Temperature and intensity ratios for the conformational study of 1-fluoro-4-pentyne dissolved in krypton solution

| *T* (°C) | 1000 (K) | *F-trans/H-trans* | | | *F-trans/Me-trans* | | |
|---|---|---|---|---|---|---|---|
| | | $I_{503/432}$ | $I_{839/1031}$ | $I_{503/1031}$ | $I_{503/533}$ | $I_{503/1291}$ | $I_{839/827}$ |
| −105 | 5.9471 | 7.912 | 2.428 | 23.008 | 5.747 | – | 0.853 |
| −110 | 6.1293 | 8.106 | 2.489 | 24.008 | 5.897 | 12.871 | – |
| −115 | 6.3231 | 8.566 | 2.695 | 25.196 | 5.997 | 13.017 | 0.900 |
| −120 | 6.5295 | 8.660 | 2.763 | 25.885 | 6.700 | 15.219 | 0.951 |
| −125 | 6.7499 | 8.976 | 2.897 | 26.336 | 7.092 | – | 1.029 |
| −130 | 6.9857 | 8.939 | 3.038 | 28.877 | 7.438 | 15.839 | 1.083 |
| −135 | 7.2385 | 9.561 | 3.124 | 31.153 | 7.874 | 16.779 | 1.180 |
| $\Delta H$ ($cm^{-1}$) | | 93 ± 10 | 141 ± 10 | 154 ± 13 | 182 ± 14 | 169 ± 34 | 179 ± 13 |

Average $\Delta H$ = 178 ± 10 $cm^{-1}$ (2.13 ± 0.10 kJ/mol) for *F-trans* to *Me-trans* from and 129 ± 9 $cm^{-1}$ (1.55 ± 0.10 kJ/mol) for *F-trans* to *H-trans* form.

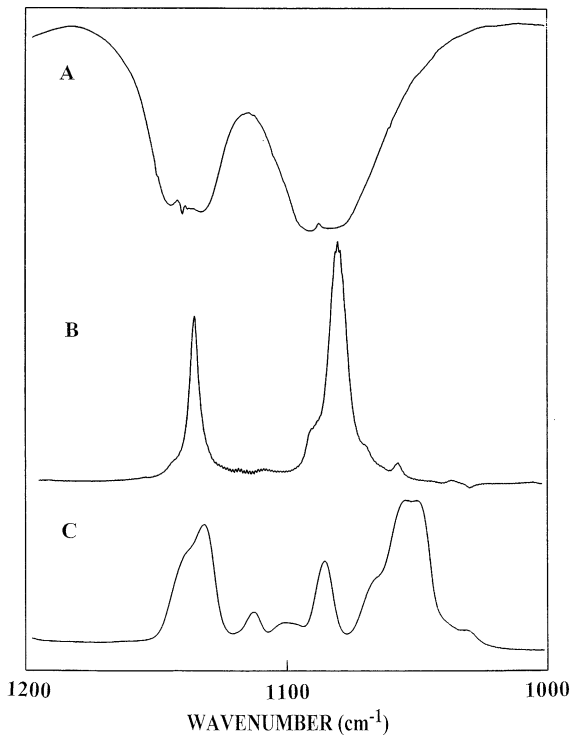


Fig. 7. Infrared spectra of 4-fluoro-1-pentyne: (A) gas; (B) krypton solution; and (C) annealed solid (1000–1200 $cm^{-1}$).

the values of 178 ± 18 $cm^{-1}$ (2.13 ± 0.21 kJ/mol) and 129 ± 13 $cm^{-1}$ (1.54 ± 0.16 kJ/mol) are considered to be more realistic values and it is expected that these values should be close to the values in the gas [5–8,20–22]. With these enthalpy differences, the amounts of the *F-trans*, *H-trans* and *Me-trans* conformers presents at ambient temperature are 51, 27 and 22%, respectively.

## 6. Discussion

The structural parameters obtained from the MP2/6-31G(d) calculations are similar for all three conformers. Most of the bond distances and angles different by very small values but there are some differences which should be noted. The CF bond distances for the *H-trans* and *Me-trans* conformers are almost the same whereas the *F-trans* conformer has a value 0.003 Å longer for this bond. This difference is probably due to the different distances between the fluorine atom and the triple bond moiety in the three conformers. The atomic arrangement also causes the $C_5H_6$ and $C_5H_7$ bond distances in the *F-trans* and *H-trans* conformers, respectively, to be shorter

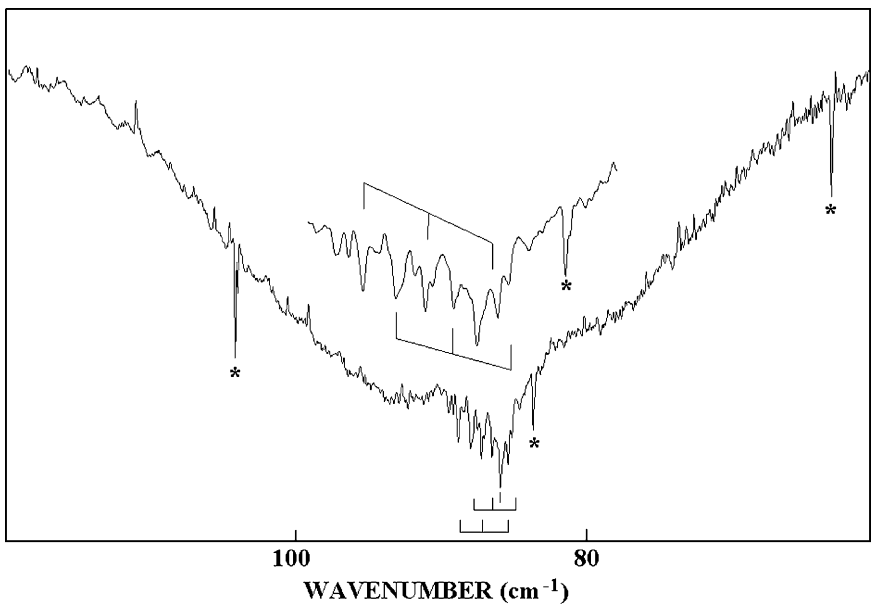


Fig. 8. Far-infrared spectrum of 4-fluoro-1-pentyne in gas phase. Asterisks indicates HCL rotational bands.

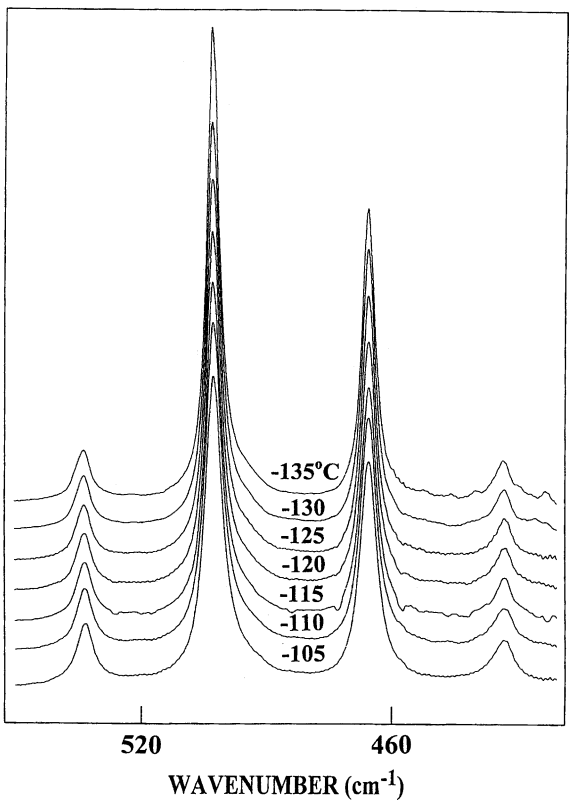


Fig. 9. Temperature dependent infrared spectrum of 4-fluoro-1-pentyne in liquid krypton solution in the temperature between − 105 and − 135 °C.

than those of the other conformer. The largest difference for the angles comes from the $\angle C_3C_4F$ in the *H-trans* and *Me-trans* conformers which is larger by 1.3 and 1.1°, respectively, than the same angle for the *F-trans* conformer. The $\angle C_3C_4C_5$ of the *H-trans* conformer is larger than that of the *Me-trans* form by 1.2° whereas the difference in this angle between the *F-trans* and *Me-trans* forms is only 0.4°. Additionally, the $\angle C_3C_4H_4$ of the *H-trans* conformer is less than that of the *F-trans* and *Me-trans* conformer by 1.1 and 1.2°, respectively. The remaining angles are essentially the same among the three conformers except for the dihedral angles $\tau_2$ and $\tau_3$.

Since most of the structural parameters are nearly the same for all these conformers, the force constants are also nearly the same. The exceptions which have significantly different values are those for the $C_2C_3C_4$ bend which is nearly 11% larger for the *H-trans* form (0.806 versus 0.720 mdyn/Å) compared to the value for the *F-trans* conformer. Also both of the hydrogen bends on carbon 3 ($H_3C_3C_4$ and $H_2C_3C_4$) have values ranging from 7.8 to 4.5% smaller for the *Me-trans* and *H-trans* conformers than the corresponding force constants for the *F-trans* form. However, only the $H_2C_3C_2$ angle bond is significantly different for the *H-trans* form where it is 5.8% larger (0.580 versus 0.548 mdyn/Å) than the corresponding one for the *F-trans* rotamer. There is also a significant decrease (more than 5.0%) in the $C_3C_2C_1$ bending force constants for both the *H-trans* and *Me-trans* conformers. Both of the force constants for the H–C ≡ C bends for the *Me-trans* conformer are about 4% smaller than those for the *F-trans* from and the 'out-of-plane' one for the *H-trans* form is 3% smaller. Since so few of the force constants have different values only a very few of the normal modes have significant differences in their vibrational frequencies among the three conformers. Most of these differences result from the differences in the mixing of the symmetry coordinates of the three conformers rather than differences in the values of the force constants.

The P.E.D.s are relatively pure for a molecule without any symmetry elements and the two 'substituents' the methyl group and the fluorine atom have similar masses. For the *F-trans* conformer, only the $CH_3$ rock ($\nu_{19}$) and $C_2C_3C_4$ bend ($\nu_{26}$) have significant contributions from four different symmetry coordinates. These two modes along with the other $CH_3$ rock ($\nu_{21}$) have only contributions of 22–24% for the indicated motions. Also the fundamental at 1080 $cm^{-1}$ (CF stretch, $\nu_{18}$) has only 37% contribution of $S_{18}$. For the other conformers, particularly the *H-trans* form, the mixing is slightly greater with four of the modes having major contributions from four symmetry coordinates with only a maximum contribution of 15% for anyone symmetry coordinated for the CF stretch ($\nu_{18}$). Nevertheless with these few exceptions the designed vibrational descriptions reflect reasonably well the major molecular motions contributing to the assigned fundamentals.

It should be noted that the infrared bands arising from the CF stretching fundamental shift to lower frequency in the spectrum of the annealed solid (Fig. 7). This fundamental is assigned at 1080 and 1081 $cm^{-1}$ in the spectra of gas and krypton solution, respectively, which moves to 1065 $cm^{-1}$ in the solid state. We frequently observed about 15–25 $cm^{-1}$

shifts for the corresponding fundamental of similar molecules [9,23,24]. It is believed that the weak interaction of the fluorine atom with adjacent molecules weakens the force constant of the CF bond and consequently, lowers the CF fundamental frequencies in the solid.

The experimental potential function (Fig. 10) governing the conformer internal rotation was determined by utilizing the two experimental $\Delta H$ values from the krypton solution, the observed torsional transitions of the three conformers and the dihedral angle of the *F-trans* form from the MP2/6-311 + G(d,p) calculation. All of these data were used to fit an asymmetric potential function of the type:

$$V(\phi) = \sum_{i=1}^{3}\left(\frac{V_i}{2}\right)(1 - \cos i\phi) + \sum_{i=1}^{3}\left(\frac{V_i'}{2}\right)\sin i\phi$$

where $\phi$ and $i$ are the torsional angle and foldness of the barrier, respectively.

A series of torsional transitions were observed in the far infrared spectrum of gas for all three conformers (Fig. 8). However, their assignments are rather difficult and in some cases rather tentative. Since the fundamental of the *Me-trans* conformer will be the 'highest' in the three wells, it should have the lowest frequency of the three fundamentals for three conformers. One series appears to begin at 87.8 but the successive bands in the spectrum (Fig. 8) are too close to be assigned to a single rotor. Therefore, every other one was assigned to one series with the remaining ones assigned to the second series. The series beginning with the highest frequency was assigned to the internal rotation of the *H-trans* conformer whereas the second series was assigned to the *F-trans* form since successive bands better fit the predicted frequencies from the determined potential function. However, the assignment could probably be reversed without a significant degrading of the determined potential parameters. Thus, the torsional fundamental for the *F-trans*, *H-trans* and *Me-trans* conformers are assigned at 87.8, 88.6 and 85.7 $cm^{-1}$, respectively. Two additional excited state transitions for the *F-trans* and *H-trans* conformers fall to lower frequency and all of these peaks and their assignments are listed in Table 8. With these assignments, a potential function governing internal rotation has been calculated and for comparison, the predicted potential function was obtained from the MP2/6-31G(d) calculations. The predicted and experimental determined plots are shown in Fig. 9 and the potential coefficients of the cosine terms, $V_1$ to $V_6$ and those for

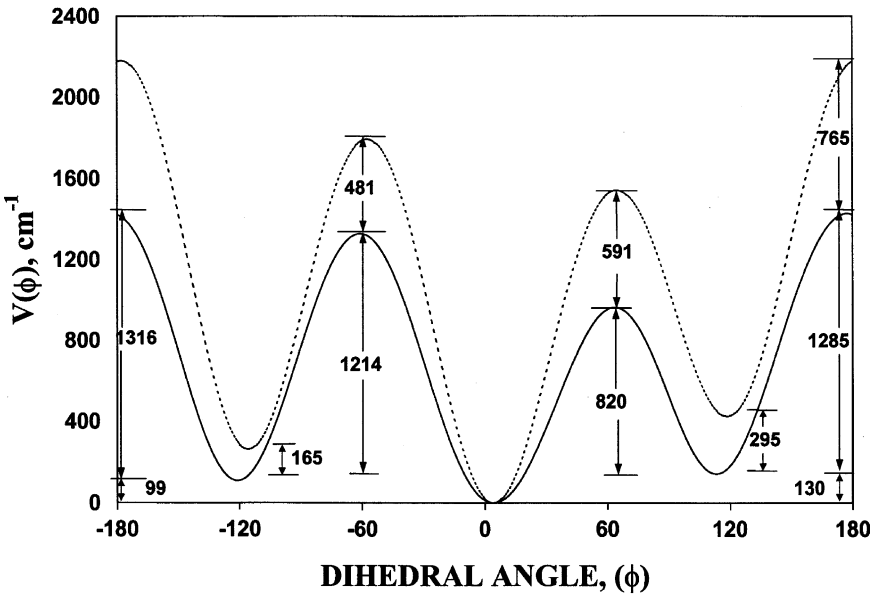


Fig. 10. Potential function governing the internal rotation of 4-fluoro-1-pentyne as determined by ab initio calculations (MP2/6-31(d), dotted line) and determined from far infrared spectrum with the value of the lowest energy point $-11$ $cm^{-1}$ and phase shift 180°.

Table 8
Far infrared torsional transitions ($cm^{-1}$) of gaseous 4-fluoro-1-pentyne

| Conformer | Transition | Obs. | Calc.[a] | Obs. − calc. |
|---|---|---|---|---|
| *F-trans* | 1 ← 0 | 87.75 | 88.64 | −0.89 |
| | 2 ← 1 | 86.24 | 86.64 | −0.40 |
| | 3 ← 2 | 84.80 | 84.58 | 0.22 |
| *H-trans* | 1 ← 0 | 88.60 | 88.74 | −0.14 |
| | 2 ← 1 | 86.98 | 86.92 | 0.06 |
| | 3 ← 2 | 85.10 | 85.06 | 0.04 |
| *Me-trans* | 1 ← 0 | 85.66 | 85.62 | 0.04 |

[a] Calculated using the potential coefficients listed in Table 9.

the sine terms $V'_1$ to $V'_6$ are listed in Table 9. In the final fit the $V_4, V_5$ and $V_6$ cosine terms were fixed as well the $V'_4, V'_5$ and $V'_6$ sine terms, all of which are quite small. The agreements between the predicted and experimentally determined potential coefficients and potential function are considered satisfactory except for the $V'_3$ term. Both potential functions show that the energy barrier between the *Me-trans* and *F-trans* conformers is higher than the barrier between the *H-trans* and *F-trans* rotamers. This result is considered reasonable because the transition between the *H-trans* and *F-trans* conformers will generate a relatively high energy transition state with a significant steric hindrance between the methyl group and the eclipsing acetylene moiety. However, all of the predicted transitional energy barriers are larger than those of the experimental fitted results. Moreover, the experimental barrier between the *Me-trans* and *F-trans* conformers is significantly lower than that predicted by the ab initio calculations but only one transition was assigned in the Me-trans well.

For 4-fluoro-1-pentyne, there are three conformers existing in both fluid states with the *F-trans* conformer the most stable form. However, the intensity of the peaks due to the *F-trans* conformer drastically decreases in the spectra of the annealed solid. Therefore, this conformer tends to convert to either the *H-trans* or *Me-trans* form in the amorphous solid. Based on the MP2/6-31G(d) calculations, the dipole moment of the *F-trans* conformer is predicted as 1.642 D which is about 0.5 D less than those of the other two conformers and the *H-trans* form has the smallest molecular volume with the $a_0$ value of 3.8 Å. These differences are expected to have a significant effect on the conformer distributions as well as

Table 9
Potential barriers ($cm^{-1}$) and coefficients ($cm^{-1}$) of 4-fluoro-1-pentyne determined from far infrared spectra and from ab initio calculations

| Coefficients | Experimental[a,b] | MP2/6-31G(d) |
|---|---|---|
| $V_1$ | 322 ± 47 | 571 |
| $V_2$ | −78 ± 45 | −138 |
| $V_3$ | 1132 ± 11 | 1584 |
| $V_4$ | −21 | 16 |
| $V_5$ | −45 | −1 |
| $V_6$ | 9 | 33 |
| $V'_1$ | −189 ± 7 | −87 |
| $V'_2$ | −286 ± 13 | −208 |
| $V'_3$ | 51 ± 21 | −217 |
| $V'_4$ | −30 | 27 |
| $V'_5$ | −14 | −16 |
| $V'_6$ | 23 | – |
| $\Delta H/\Delta E$ (*F-trans* → *H-trans*) | 110 ± 13 | 264 |
| $\Delta H/\Delta E$ (*F-trans* → *Me-trans*) | 140 ± 18 | 425 |
| Potential barriers | | |
| *F-trans* → *H-trans* | 1324 | 1794 |
| *F-trans* → *Me-trans* | 961 | 1541 |
| *H-trans* → *F-trans* | 1214 | 1530 |
| *Me-trans* → *F-trans* | 820 | 1116 |
| *H-trans* → *Me-trans* | 1315 | 1916 |
| *Me-trans* → *H-trans* | 1285 | 1755 |
| Dihedral angle[c] (*F-trans*) | 4.18 | 4.08 |

[a] Calculated using: $F_0 = 0.757194$, $F_1 = 0.111219$, $F_2 = 0.049529$, $F_3 = 0.005586$, $F_4 = 0.003244$; $F_5 = 0.000326$, $F_6 = 0.000221\ cm^{-1}$ and $F'_1 = -0.0036087$, $F'_2 = -0.001677$, $F'_3 = -0.000256$; $F'_4 = -0.000186$, $F'_5 = 0.000003$, $F'_6 = -0.000018\ cm^{-1}$.
[b] Values for $V_4, V_5$ and $V_6$ and $V'_4, V'_5$ and $V'_6$ are fixed.
[c] Phase shifts 180°.

the molecular packing in the solid state. No polycrystalline solid with only one conformer could be obtained in this study and all spectra of the solid show the coexistence of three conformers but with a significant less amount of the *F-trans* form than found in the fluid states. This observation can possibly be explained by the potential function of the conformational interconversion (Fig. 10). The energy barrier between the *F-trans* and *Me-trans* conformers is less than $1000\ cm^{-1}$ whereas the *F-trans* to *H-trans* barrier is slight higher than $1300\ cm^{-1}$. Therefore, the *F-trans* conformer is more likely to convert to the *Me-trans* form first rather than to the *H-trans* form. However, the *H-trans* form could be more stable than the *Me-trans* in the solid state because of a lower enthalpy of about $50\ cm^{-1}$ as well as its smaller

molecular volume. This appears to be confirmed by comparing the infrared bands at 535 and 433 $cm^{-1}$ ($\nu'_{26}$, $\nu''_{27}$) which arise from the *Me-trans* and *H-trans* forms, respectively, in the spectra of the gas and solid where the later one shows a slightly increased intensity (Fig. 4) with annealing. The thermal motion at such a low temperature may not provide enough energy to support this transition. Therefore, the conformer interconversion is very slow and consequently, the bands due to all three conformers are observed in the spectra of the solid states.

In the previous study of 4-fluoro-1-butyne [9] which is similar to 4-fluoro-1-pentyne with the only difference the substitution of a hydrogen atom by the methyl group, the *trans* conformer is found to be the more stable form with an enthalpy difference of 212 $cm^{-1}$. However, for 4-fluoro-1-butyne, the *gauche* form is the only conformer in the crystalline solid. The predicted dipole moment of the *gauche* conformer is about 0.68 D larger than that of the *trans* form whereas the *trans* to *gauche* energy barrier is 1142 $cm^{-1}$ which is slightly less than that of 4-fluoro-1-pentyne. Therefore, a larger difference in dipole moment along with a lower potential barrier apparently benefits the formation of the pure conformer in the crystalline solid for 4-fluoro-1-butyne.

For 1-pentyne [1,4] the *trans* conformer with the methyl group *trans* to the triple bond is more stable than the *gauche* conformer. But for 4-fluoro-1-pentyne, the *F-trans* conformer becomes more stable than the *Me-trans* conformer by 178 $cm^{-1}$. Since the size of the methyl group is larger than that of the fluorine atom, the steric factor cannot be the main cause for this difference. In the previous study of 4-fluoro-1-butyne [9], the shorter $C_3C_4$ bond distance comparing with that of 1-fluoropropane [24] is believed as one of the key factors which causes the *trans* form to be more stable than the *gauche* conformer. Therefore, the variation of the $C_3C_4$ bond distance is strongly correlated to the change of the conformational stability. The $C_3C_4$ bond distance in the *Me-trans* conformer of the fluoropentyne is about 0.010 Å shorter than that of the *trans* form of 1-pentyne as predicted by MP2/6-31G(d) calculations which further supports this assumption. Thus, it appears that the $C_3C_4$ bond distance significantly affects the conformational stability of these pentyne derivatives.

Although the ab initio calculations at all levels predicted the *F-trans* form as the most stable conformer which is consistent with the experimental investigation, the DFT calculations at B3LYP/DZ(d), B3LYP/DZ(d, p) and B3LYP/cc-pVDZ basis sets give incorrect predictions on the conformational stabilities for the *H-trans* and *Me-trans* forms with the latter one more stable by 13, 24 and 47 $cm^{-1}$, respectively (Table 4). Additionally, the predicted energy difference from the RHF/6-31G(d) calculations is only 4 $cm^{-1}$ which is much smaller than the experimental values. However, all MP2 calculations gave the correct predictions with the energy differences ranging from 100 to 205 $cm^{-1}$ between these two conformers. Therefore, the theoretical predictions by RHF and DFT calculations with

Table 10
Predicted and experimental determined conformational stabilities of 4-fluoro-1-pentyne and other similar molecules

| Molecules | | Ab initio/DFT predictions | | | | Experimental results[a] |
|---|---|---|---|---|---|---|
| | | RHF/6-31G(d) | B3LYP/6-31G(d) | MP2/6-31G(d) | MP2/6311G(2d,2p) | |
| 4-Fluoro-1-butyne | | 444 | 362 | 290 | 358 | 215 |
| 4-Chloro-1-butyne | | 512 | 450 | 389 | 317 | 147 |
| 5-Fluoro-2-pentyne | | 460 | 375 | 312 | 420 | 272 |
| 5-Chloro-2-pentyne | | 518 | 451 | 393 | 328 | 233 |
| 1-Pentyne | | 107 | 33 | −122 | -131 | 50 |
| 2-Hexyne | | 58 | 26 | −148 | 154 | 74* |
| 4-Fluoro-1-pentyne | *F-trans/Me-trans* | 641 | 398 | 429 | 503 | 178* |
| | *F-trans/H-trans* | 637 | 387 | 269 | 357 | 129* |

Negative signs indicated the *gauche* form more stable.
[a] Experimental results come from xenon or krypton solutions.

various basis set do not give clear predictions as those from MP2 calculations.

It is interesting to compare the conformational stabilities predicted from the ab initio calculations with the corresponding experimental results for some butyne derivatives (Table 10). [4,9,23,25–27] For these halo-substituted derivatives, including 4-halo-1-butyne and 5-halo-2-pentyne, the ab initio calculations give the correct predictions where the experimental determined enthalpy difference is larger than 150 $cm^{-1}$. The values of enthalpy difference are smaller for the pure hydrocarbon molecules such as 2-hexyne and 1-pentyne. Based on these studies, one can expect that the *halo-trans* form is more stable than *methyl-trans* form when both of them coexist and this is confirmed by the study of 4-fluoro-1-pentyne. Whether ab initio calculations can provide the correct predictions for the conformational stability of a molecule largely depends on the energy difference between the two conformers which is clearly shown in Table 10. For example, the experimentally determined $\Delta H$ and calculated energy difference (MP2/6-311G(2d,2p)) for 2-hexyne [27] are 74 and 154 $cm^{-1}$, respectively, where the MP2/6-31G(d) calculations give the wrong prediction. Furthermore, for 1-pentyne, even the MP2/6-311 + G(2df,2pd) calculations do not give the correct prediction with the experimentally determined enthalpy value of 50 $cm^{-1}$. Thus, the predictions from the theoretical calculations can be problematic when the calculated energy differences are than 150 $cm^{-1}$ and such predictions need to be verified by experimentally determined results.

## Acknowledgements

J.R. Durig acknowledges the University of Missouri-Kansas City Faculty Research Grant program for partial support of these studies.

## References

[1] S. Bell, G.A. Guirgis, Y. Li, J.R. Durig, J. Phys. Chem. A 101 (1997) 5987.
[2] W.A. Herrebout, B.J. van der Veken, A. Wang, J.R. Durig, J. Phys. Chem. 99 (1995) 578.
[3] M. Traetteberg, P. Bakken, H. Hopt, J. Mol. Struct. 509 (1999) 213.
[4] J.R. Durig, B.R. Drew, J. Mol. Struct. 509 (2001) 247.
[5] M.O. Bulanin, J. Mol. Struct. 19 (1973) 59.
[6] B.J. van der Veken, E.R. DeMunck, J. Chem. Phys. 97 (1992) 3060.
[7] M.O. Bulanin, J. Mol. Struct. 347 (1995) 73.
[8] W.A. Herrebout, B.J. van der Veken, J. Phys. Chem. 100 (1996) 9671.
[9] G.A. Guirgis, X. Zhu, S. Bell, J.R. Durig, J. Phys. Chem. A 105 (2001) 363.
[10] C. Moller, M.S. Plesset, Phys. Rev. 46 (1934) 618.
[11] K. Furic, J.R. Durig, Appl. Spectrosc. 42 (1988) 175.
[12] F.A. Miller, B.M. Harney, Appl. Spectrosc. 24 (1970) 291.
[13] M.J. Frisch, G.W. Trucks, H.B. Schlegel, G.E. Scuseria, M.A. Robb, J.R. Cheeseman, V.G. Zakrzewski, J.A. Montgomery, R.E. Stratmann, J.C. Burant, S. Dapprich, J.M. Millam, A.D. Daniels, K.N. Kudin, M.C. Strain, O. Farkas, J. Tomasi, V. Barone, M. Cossi, R. Cammi, B. Mennucci, C. Pomelli, C. Adamo, S. Clifford, J. Ochterski, G.A. Petersson, P.Y. Ayala, Q. Cui, K. Morokuma, D.K. Malick, A.D. Rabuck, K. Raghavachari, J.B. Foresman, J. Cioslowski, J.V. Ortiz, B.B. Stefanov, G. Liu, A. Liashenko, P. Piskorz, I. Komaromi, R. Gomperts, R.L. Martin, D.J. Fox, T. Keith, M.A. Al-Laham, C.Y. Peng, A. Nanayakkara, C. Gonzalez, M. Challacombe, P.M.W. Gill, B.G. Johnson, W. Chen, M.W. Wong, J.L. Andres, M. Head-Gordon, E.S. Replogle and J.A. Pople, Gaussian 98 (Revision A.7) Gaussian, Inc., Pittsburgh PA, 1998.
[14] P. Pulay, Mol. Phys. 17 (1969) 197.
[15] G.A. Guirgis, X. Zhu, Z. Yu, J.R. Durig, J. Phys. Chem. A 104 (2000) 4383.
[16] R.D. Amos, Chem. Phys. Lett. 124 (1986) 376.
[17] M.J. Frisch, Y. Yamaguchi, J.F. Gaw, H.F. Schaefer, J.S. Berkley, J. Chem. Phys. 84 (1986) 531.
[18] G.W. Chantry, in: A. Anderson (Ed.), The Raman Effect, vol. 2, Marcel Dekker, New York, 1971.
[19] J.M. Frish, Y. Yamagushi, J.F. Gaw, H.F. Schaefer III, J.S. Binkley, J. Chem. Phys. 84 (1986) 531.
[20] P.L. Polavarapu, J. Chem. Phys. 94 (1990) 8106.
[21] R.D. Amos, Phys. Lett. 124 (1986) 374.
[22] W.A. Herrebout, B.J. van der Veken, A. Wang, J.R. Durig, J. Phys. Chem. 99 (1995) 578.
[23] S. Bell, X. Zhu, G.A. Guirgis, J.R. Durig, J. Phys. Chem. Chem. Phys. 3 (2001) 776.
[24] G.A. Guirgis, X. Zhu, J.R. Durig, Struct. Chem. 10 (1999) 445.
[25] J.R. Durig, B.R. Drew, G.A. Guirgis, J. Raman Spectrosc. 32 (2001) 757.
[26] G.A. Guirgis, B.R. Drew, J.J. Luangjamekorn, S. Shen, J.R. Durig, J. Mol. Struct. 613 (2001) 15.
[27] S. Bell, X. Zhu, G.A. Guirgis, J.R. Durig, J. Mol. Struct. 616 (2002) 135.